Kinetic Mechanism and Cofactor Content of Soybean Root Nodule Urate Oxidase†

Kalju Kahn and Peter A. Tipton*

Department of Biochemistry, University of Missouri—Columbia, Columbia, Missouri 65211

Received December 12, 1996; Revised Manuscript Received February 20, 1997⊗

ABSTRACT: The kinetic mechanism of urate oxidase isolated from soybean root nodules has been determined by initial velocity kinetic studies monitoring oxygen uptake, in order to avoid potential artifacts in the spectrophotometric assay which arise from absorbance due to unidentified products of the enzymatic reaction. Urate and O_2 bind to the enzyme sequentially; xanthine is a competitive inhibitor versus urate and a noncompetitive inhibitor versus O_2, which suggests that urate binds to the enzyme before O_2. This kinetic mechanism was confirmed by an ^{18}O isotope-trapping experiment, which demonstrated that O_2 does not bind productively to the enzyme in the absence of urate. The pH dependence of V and $(V/K)_{urate}$ reveal the presence of an ionizable residue on the enzyme with a pK of ∼6.2, which must be unprotonated for the catalytic reaction to occur. The $(V/K)_{O_2}$ profile is pH independent; these data are accomodated by a model in which a unimolecular step intervenes between the binding of urate and O_2. The pK_i profile for 9-methylurate, a competitive inhibitor versus urate, is pH independent, confirming that the protonation state of the ionizable residue is not important for binding. The pK_i profile for xanthine defines a pK of 7.4, which demonstrates that the monoanion of xanthine binds to the enzyme; by analogy, the monoanion of urate is predicted to be the substrate. The four isomeric *N*-methylurates were examined as potential inhibitors of urate oxidase. Only 9-methylurate showed significant inhibition suggesting that ionization at N9 of urate is not required for binding; it is proposed that the N3-deprotonated urate monoanion is the species which binds to urate oxidase. The gene encoding urate oxidase was cloned from soybeans and expressed in *Escherichia coli*. The metal content of the recombinant enzyme was examined by inductively coupled argon plasma emission spectroscopy, and only trace quantities of copper were found. The molecular mass of the protein was determined by MALDI-TOF mass spectrometry and found to be 35 059.8 Da. The calculated molecular mass of urate oxidase is 35 052 Da; therefore, these data suggest that there is no covalently bound cofactor in urate oxidase.

Urate oxidase is a widely occurring enzyme which catalyzes the oxidation of urate with the concomitant reduction of O_2 to H_2O_2. The metabolic role fulfilled by this reaction varies among different organisms. The presence of urate oxidase allows some bacteria, such as *Bacillus fastidiosus*, to grow on urate as the sole carbon and nitrogen source (Kaltwasser, 1971). In most mammals, urate oxidase functions in the pathway by which excess nitrogen is excreted. Interestingly, humans and other higher primates do not have a functional urate oxidase as a result of mutations within the coding sequence of the gene (Wu et al., 1992). It has been suggested that the lack of urate oxidase confers a selective advantage because it leads to increased serum urate levels and urate may be a physiologically important antioxidant (Ames et al., 1981; Sevanian et al., 1991). In tropical leguminous plants, such as soybean (*Glycine max*), urate oxidase functions in the nitrogen assimilation pathway. Nitrogen, which is fixed in the root nodules through the action of the bacterial symbiont's nitrogenase, is used for *de novo* purine biosynthesis; oxidation of purines catalyzed by xanthine dehydrogenase and urate oxidase leads to the formation of ureides, which are the metabolites that carry nitrogen throughout the plant (Reynolds et al., 1982). In nodulated soybean plants, 78% of the total nitrogen in the xylem sap was found in the form of ureides (McClure & Israel, 1979) and ureides have been estimated to account for 35−50% of the nitrogen entering the soybean pod (Layzell & LaRue, 1982). Flux through the ureide pathway is critical for nitrogen fixation and metabolism. Inhibition of xanthine dehydrogenase, which catalyzes the step preceding that of urate oxidase, in intact cowpea root nodules led to decreased nitrogenase activity, although the mechanism of this interaction remains unknown (Atkins et al., 1988). Plants in which urate oxidase activity was reduced by 80% through expression of antisense urate oxidase RNA showed symptoms of nitrogen deficiency and had nodules that were reduced in size (Lee et al., 1993).

Studies of the urate oxidase reaction began in the 1930s (Schuler & Reindel, 1933; Keilin & Hartree, 1936); despite its long history and metabolic importance, the properties of the enzyme and its catalytic reaction remain obscure. The identity of the true product of the enzymatic reaction long remained unknown. Although allantoin appears to be the ultimate product of urate oxidase action upon urate, absorption spectroscopy and NMR studies suggest that the enzyme catalyzes the conversion of urate to a metastable species which decays nonenzymatically to allantoin (Bongaerts & Vogel, 1979; Modric et al., 1992); recent work suggests that this species is 5-hydroxyisourate.[1] The pig liver urate oxidase was first characterized as a copper-dependent enzyme

† Supported by USDA Grant 94-37305-0578.

* To whom correspondence should be addressed. Telephone: (573) 882-7968. Fax: (573) 884-4812. E-mail: bctipton@muccmail.missouri.edu.

⊗ Abstract published in *Advance ACS Abstracts,* April 15, 1997.

[1] K. Kahn and P. A. Tipton, manuscript submitted.

S0006-2960(96)03184-4 CCC: $14.00

(Mahler et al., 1955). However, copper has never been found in stoichiometric amounts in any urate oxidase, and urate oxidase from bacteria (Bongaerts et al., 1978), yeast (Nishimura et al., 1982), and fungi (Conley & Priest, 1980a) have been shown to be metal-free. The soybean root nodule enzyme was reported to contain 0.76 equiv of copper per tetrameric holoenzyme (Bergmann et al., 1983). There is no evidence for the presence of an organic cofactor in urate oxidase, so the mechanism through which the O_2-dependent chemistry occurs remains an intriguing question.

As a prelude to mechanistic studies of urate oxidase, we have examined its steady-state kinetic properties and reexamined the metal content. Earlier kinetics studies have yielded equivocal results. It was reported that the porcine liver urate oxidase reaction was characterized by nonlinear reciprocal plots, from which it was concluded that the enzyme followed a steady-state random mechanism (Pitts & Priest, 1974). In contrast, investigations of urate oxidase from *Aspergillus flavus* failed to demonstrate binding of O_2 to free enzyme (Conley & Priest, 1980b), which implies an ordered mechanism for substrate addition. These studies relied on spectrophotometric assays to monitor the enzymatic reaction. However, the fact that urate oxidase releases a metastable species whose absorbance spectrum is quite similar to that of urate (Bongaerts & Vogels, 1979) renders the spectrophotometric assay of urate oxidase unreliable, so it is not clear whether the conflicting results of earlier kinetic studies resulted from differences between the enzymes isolated from different sources or are the results of the experimental methods used. We have sought to characterize the catalytic reaction of the soybean root nodule enzyme by following O_2 uptake with an oxygen electrode, which avoids the complications inherent in the spectrophotometric assay. The initial velocity kinetic studies reported here define the order of substrate addition as well as the state of protonation of the enzyme and the substrate required for reaction, which have not been defined previously. We have also examined the metal content of purified urate oxidase as well as the effects of copper and copper chelating agents on the activity of the enzyme.

MATERIALS AND METHODS

Urate, xanthine, 1-methylurate, 3-methylurate, 7-methylurate, and 9-methylurate were purchased from Sigma Chemical Co. and were used without further purification. Xanthine−agarose and catalase were also purchased from Sigma. Authentic menadione epoxide was synthesized by literature procedures (Snatzke, 1980). $^{18}O_2$ (95 −98 at. %) was purchased from Cambridge Isotope Labs.

Purification of Soybean Root Nodule Urate Oxidase. Urate oxidase was purified from soybean root nodule extracts (Karr et al., 1984) which was generously supplied by Professor David Emerich. All operations were performed at 4 °C. Typically, 50 mL of extract was brought to 25% saturation by addition of solid ammonium sulfate, and the precipitated protein was removed by centrifugation. The supernatant was brought to 50% saturation by further addition of ammonium sulfate. Following centrifugation, the protein pellet was dissolved in a minimum volume of 20 mM Tris, pH 7.4, containing 1 mM DTT[2] and 0.01% (v/v) Triton X-100. The material was dialyzed overnight against the same buffer, and insoluble material was removed by centrifugation. The supernatant was applied to a xanthine−agarose column (1.5 × 11 cm) equilibrated in 20 mM Tris, pH 7.4, and the column was washed with the same buffer until the absorbance of the effluent at 280 nm returned to baseline. Urate oxidase was eluted from the column by washing it with 20 mM Tris, pH 7.4, containing 0.5 mM xanthine.

Fractions containing urate oxidase were pooled and dialyzed against 20 mM Tris, pH 7.4, overnight. After dialysis, the enzyme was concentrated by placing the dialysis bag on a bed on PEG 20000 for several hours until protein precipitate was visible. The suspension was dialyzed against 20 mM Tris, pH 8.5, for several hours, during which time the precipitated protein redissolved. Enzyme stored at 4 °C was active for several weeks.

Enzyme Assays. Urate oxidase activity was routinely measured by two methods. During the purification, enzyme activity was determined by monitoring the disappearance of urate at 292 nm with a Hewlett-Packard 8452A spectrophotometer. Standard assays conditions were 0.1 mM urate in air-saturated 100 mM CHES, pH 9.25. For kinetic studies, the reaction was monitored by following the disappearance of O_2 from solution with a YSI Model 5300 Biological Oxygen monitor equipped with a 0.6 mL microchamber. The temperature of the microchamber was maintained at 25 °C with a circulating water bath. Reactions were initiated by the addition of enzyme (typically 10 μL), and the analog signal from the O_2-electrode was digitized and collected at a rate of 2 Hz. The data acquisition and analysis was accomplished using LabView software (National Instruments) running on a PowerMac 7100.

O_2 concentrations were varied by saturating urate solutions with O_2/N_2 gas mixtures (Matheson) in which the O_2 concentrations were 50, 80, or 140 μM, or by mixing together O_2-saturated and N_2-saturated solutions in the appropriate proportions to yield the desired O_2 concentration. The range of O_2 concentrations used was 50−740 μM. The O_2 concentration in air-saturated buffers was 270 μM. Urate solutions were prepared fresh daily, and their concentrations were determined spectrophotometrically (ϵ_{292}, 12 300 cm^{-1} M^{-1}). Experiments in which urate was the varied substrate were conducted in buffers in which the O_2 concentration was 480 μM, except where noted. The following buffers were used at 100 mM in the pH ranges indicated: MOPSO, pH 5.75−6.25; MES, pH 6.25−6.5; HEPES, pH 6.5−8.0; TAPS, pH 8.5; CHES, pH 9.0−10.0. To determine the pH dependence of K_i for xanthine and 9-methylurate, full inhibition patterns were obtained at the extremes of the pH range examined, and Dixon plots (Segel, 1975) were used to determine K_i at intermediate pH values. These experiments were conducted in air-saturated buffers. Xanthine and 9-methylurate were competitive inhibitors versus urate under all of the conditions examined.

Data Analysis. Initial velocities were determined from linear regression analysis of the time courses, and the data were fitted to the appropriate equations by nonlinear least-

[2] Abbreviations: CHES, 2-(*N*-cyclohexylamino)ethanesulfonic acid; DTT, dithiothreitol; HEPES, *N*-(2-hydroxyethyl)piperazine-*N*′-2-ethanesulfonic acid; IPTG, isopropyl β-D-thiogalactopyranoside; MES, 2-(*N*-morpholino)ethanesulfonic acid; MOPSO, 3-(*N*-morpholino)-2-hydroxypropanesulfonic acid; TAPS, 3-[[tris(hydroxymethyl)methyl]amino]-propanesulfonic acid; GC−MS, gas chromatography−mass spectrometry; MALDI-TOF mass spectrometry, matrix-assisted laser desorption ionization time-of-flight mass spectrometry.

squares methods (Cleland, 1979). The data were fitted to eqs 1 or 2 when one or two substrate concentrations were varied, respectively. In these equations, *A* and *B* are the substrate concentrations, *V* is the maximal velocity, K_a and K_b are the Michaelis constants for *A* and *B*, respectively, and K_{ia} is the dissociation constant of A from the EAB complex.

$$v = \frac{VA}{K + A} \tag{1}$$

$$v = \frac{VAB}{K_aB + K_bA + AB + K_{ia}K_b} \tag{2}$$

Competitive inhibition data were fitted to eq 3, and noncompetitive inhibition data were fitted to eq 4.

$$v = \frac{VA}{K(1 + I/K_i) + A} \tag{3}$$

$$v = \frac{VA}{K(1 + I/K_{is}) + A(1 + I/K_{ii})} \tag{4}$$

The pH dependence of the kinetic parameters were fitted to eq 5, which describes a decrease in the measured parameter upon protonation of a single ionizable residue; *Y* is the parameter measured (*V*, *V*/*K*, or 1/K_i), and *C* is its pH-independent value.

$$\log Y = \log\left(\frac{C}{1 + H/K_a}\right) \tag{5}$$

^{18}O Isotope Trapping. An ^{18}O isotope-trapping experiment was conducted to determine whether O_2 could bind productively to urate oxidase in the absence of urate. The isotopic composition of the H_2O_2 produced in the enzymatic reaction was determined by using it to epoxidize menadione (Ortiz de Montellano & Catalano, 1985). The isotopic composition of the resulting menadione epoxide was determined by GC−MS analysis performed at the University of Missouri Agricultural Experiment Station. The trapping experiment was conducted as follows. A 5 mL solution of 28 μM urate oxidase was degassed by repeated cycles of evacuation and flushing with N_2. To the degassed enzyme solution was added 0.4 mL of 10 mM CHES pH 9.0 containing 1.4 mM $^{18}O_2$. This solution was added to 24 mL of vigorously stirring buffer containing 1.4 mM $^{16}O_2$ and 210 μM urate. A 2 mL aliquot was immediately removed for later analysis, and the remainder of the reaction was quenched by the addition of 3 mL of concentrated perchloric acid. Control experiments established that this method was effective in quenching the urate oxidase reaction. The quenching occurred approximately 1 s after the enzyme−$^{18}O_2$ solution was added to the urate−$^{16}O_2$ solution. We estimate that under these conditions only one or two catalytic cycles should have occurred. The quenched reaction was heated at 70 °C for 10 min, and precipitated material was removed by centrifugation. The solution was adjusted to pH 11 by the addition of solid Na_2CO_3 and added to 25 mL of warm ethanol containing 10 μmol of menadione. The reaction was incubated at 30 °C for 10 min, and the solvent was removed by rotary evaporation. The residue was extracted twice with 3 mL of diethyl ether. The ether extracts were combined, and the solvent was removed by rotary evaporation. The residue was dissolved in 0.3 mL diethyl ether and analyzed by GC−MS. The 2 mL aliquot which had been removed before the perchloric acid quench was allowed to react for 5 min. It was then quenched and worked up in the same manner as the single-turnover sample. A control reaction was conducted using a catalytic amount of urate oxidase and $^{18}O_2$ in order to prepare a sample of [^{18}O]menadione epoxide.

Cloning and Expression of the Urate Oxidase Gene. Soybean root nodules which had been stored at −80 °C were pulverized with a chilled mortar and pestle. Total RNA was extracted using the RNAzol B kit (Tel-Test, Inc.) following the manufacturer's instructions. The mRNA was reverse transcribed and amplified using the SuperScript preamplification system (Gibco BRL Life Technologies) using DNA primers that were designed based on the published sequence of soybean root nodule urate oxidase (Suzuki and Verma, 1991) and which incorporated an *Eco*RI site at the 5′ end of the amplified sequence and a *Hin*dIII site at the 3′ end. The amplified product was digested with *Eco*RI and *Hin*dIII and cloned into the pGEM 3Zf(+) vector. The insert containing the urate oxidase gene was subsequently subcloned into pBluescript SK(+), and both strands were sequenced by the dideoxy method using AmpliTaq DNA polymerase and an Applied Biosystems automated DNA sequencer. After the identity of the insert was confirmed, it was amplified using primers which incorporated an *Nde*I site and a *Bam*HI site at the 5′ and 3′ ends, respectively. The amplified product was then subcloned into the pET3-a vector (Novagen), which is a T7 promoter-based expression vector. This construct was designated pUO3. Both strands of the insert were resequenced to confirm that no mutations had been introduced by the amplification procedure. BL21(DE3) cells were transformed with pUO3 and were subsequently used for the expression of the urate oxidase gene.

For production of urate oxidase, cells were grown at 37 °C in Luria−Bertini media containing 100 μg/mL ampicillin. When the cultures reached an optical density at 600 nm of 0.5−0.6, protein expression was induced by the addition of IPTG to a final concentration of 0.4 mM. Cells were harvested by centrifugation after 3.5−4 h, washed in 50 mM Tris, pH 8.0, containing 2 mM EDTA, and stored at −80 °C.

Purification of Recombinant Urate Oxidase. Cells which had been grown as described above were resuspended in 3−4 mL/g of cell paste in 20 mM Tris, pH 8.0, containing 1 mM DTT, 1 mM EDTA, 0.01% Triton X-100, 10 μg/mL DNase I, and 0.2 mg/mL lysozyme, and stirred at room temperature for 1 h. The suspension was sonicated briefly to reduce its viscosity and centrifuged at 15000*g* for 15 min. Protamine sulfate (5 mg/g of cell paste) dissolved in water was added dropwise to the cell-free extract. The solution was centrifuged as above, and the supernatant was brought to 60% saturation by the addition of crystalline ammonium sulfate. Precipitated protein was pelleted by centrifugation, redissolved in a small volume of 20 mM Tris, pH 8.0, containing 1 mM DTT and 0.01% (v/v) Triton X-100, and dialyzed overnight against the same buffer. The dialysate was chromatographed on xanthine−agarose in the same manner as the native enzyme; active fractions were pooled, dialyzed to remove xanthine, and concentrated by ultrafiltration using an Amicon YM10 membrane.

Metal Analysis. A 4.2 μM sample of urate oxidase purified from soybean root nodules was analyzed for copper content by inductively coupled plasma emission spectroscopy at the University of Missouri Agricultural Experiment

Table 1: Purification of Urate Oxidase from Soybean Root Nodule Extract

step	volume (mL)	activity[a] (units)	protein (mg/mL)	sp. activity (units/mg)	yield (%)	-fold purification
extract	50	12	1.2	0.20	100	1.0
ammonium sulfate	9.1	9.0	4.8	0.21	80	1.1
xanthine−agarose	4.0	8.6	0.60	3.6	72	18

[a] Activity was determined using the spectrophotometric assay described in the Materials and Methods.

Station. An 18.5 μM sample of recombinant urate oxidase was submitted to the Chemical Analysis Laboratory at the University of Georgia for analysis of 30 elements, including copper, by inductively coupled argon plasma emission spectroscopy. In each case, sample blanks consisting of the buffer against which the protein was dialyzed were analyzed as well. The concentration of each sample was determined by amino acid analysis, performed at the University of Missouri Agricultural Experiment Station.

The effects of copper and a copper chelator on the activity of soybean root nodule urate oxidase were tested by overnight dialysis of aliquots of the enzyme against 20 mM Tris, pH 8.0, containing 0.1 mM $CuSO_4$, and against 20 mM CHES, pH 9.0, containing 0.5 mM 1,10-phenanthroline. A control sample was dialyzed against 20 mM CHES, pH 9.0. The protein content of each sample was determined, and the activity was measured in air-saturated 20 mM CHES, pH 9.0, containing 0.2 mM urate, using the oxygen electrode. The activity of a sample of urate oxidase was assayed in the same way in the presence of 0.5 mM 1,10-phenanthroline.

Molecular Mass Determination. Approximately 1 mg of purified recombinant urate oxidase was lyophilized from 10 mM ammonium bicarbonate and submitted to the Washington University Mass Spectrometry Resource for MALDI-TOF mass spectrometry analysis.

Protein Sequencing. A sample of recombinant urate oxidase (0.1 mg) was submitted to the University of Missouri Protein Core for N-terminal amino acid sequence analysis.

RESULTS

Purification of Urate Oxidase. Urate oxidase was purified from soybean root nodule extracts in high yield (Table 1). Higher yields of enzyme were obtained using Tris buffer in the purification, compared with other buffers, although Tris and Cl^- appeared to inhibit the enzyme (data not shown). The purified enzyme was stored in Tris buffer, but dilution of the enzyme into the assay solutions rendered the Tris and Cl^- inhibition negligible in kinetic studies carried out in other buffers. The specific activity of the preparations used in these studies, measured at pH 9.25 in air-saturated buffer and saturating concentrations of urate, was 3.6 units/mg. The specific activity of urate oxidase purified from soybean root nodules by another procedure has been reported to be 6.8 units/mg (Lucas et al., 1983); however, it is difficult to compare these values directly. Lucas et al. (1983) monitored the reaction spectrophotometrically and reported that a 1−2 min lag preceded the attainment of the steady-state rate. The value reported in this work is derived from initial velocity measurements of the disappearance of urate. The isolated enzyme was homogeneous, as judged by the appearance of a single band in Coomassie-stained SDS−polyacrylamide gels; on the basis of its electrophoretic mobility, the subunit M_r was 33 000, in good agreement with the M_r of 35 052 derived from the deduced amino acid sequence.

Recombinant Urate Oxidase. The deduced amino acid sequence from the gene cloned from soybean root nodules differed at two positions from the published sequence. At position 242, phenylalanine was found instead of leucine, and at position 276, lysine was found in place of glutamine. It is likely that these differences are genuine and are due to the fact that a different soybean variety (Williams) was used in this work. Suzuki and Verma (1991) found 11 amino acid differences in urate oxidases from soybean variety Dare and variety Prize.

Table 2: Inhibition of Urate Oxidase[a]

variable substrate	fixed substrate	inhibitor	pattern[b]	K_{is} (μM)	K_{ii} (μM))
urate	270 μM O_2	xanthine	C	4.5 ± 0.4	
O_2	40 μM urate	xanthine	NC	11.1 ± 2.0	24.6 ± 3.8
urate	270 μM O_2	9-Me-urate	C	22.4 ± 2.1	

[a] Initial velocities were determined at 25 °C by measuring O_2 uptake. [b] C, competitive, data were fitted to eq 3; NC, noncompetitive, data were fitted to eq 4.

The recombinant enzyme was expressed at satisfactory levels in *E. coli*, so that up to 20 units of urate oxidase per liter of culture was found in the cell free extract. Expression levels were somewhat higher than this figure would indicate, because approximately one-third of the urate oxidase appeared to be insoluble and was found with the cell debris after the lysis of the cells. The specific activity of the purified recombinant enzyme was 3 units/mg. Five cycles of N-terminal amino acid sequencing were performed in order to confirm the identity of the expressed protein, and to determine whether the N-terminal methionine was present. The sequence detected was AQQEV, which matches the sequence expected on the basis of the nucleotide sequence of the gene, and demonstrates that the N-terminal methionine is not present. The molecular mass of the recombinant protein, as determined by MALDI-TOF mass spectrometry, was 35 059.8 Da, in excellent agreement with the predicted molecular mass.

Metal Content. Analysis of urate oxidase purified from soybean root nodules revealed that the protein contained 0.026 atom of copper per subunit. Urate oxidase expressed in *E. coli* and purified contained 0.097 atom of copper per subunit. Trace amounts of iron, nickel, and tungsten were detected as well, but there was no evidence for the presence of any transition metal in stoichiometric quantities. The effects of dialysis against copper or 1,10-phenanthroline and assaying in the presence of 1,10-phenanthroline are summarized in Table 3.

Reaction Stoichiometry. Using calibrated stock solutions of urate and monitoring the disappearance of O_2 with the O_2-electrode, the stoichiometry of the enzymatic reaction was shown to be 0.98 ± 0.04 mol of urate oxidized per mole of O_2 (data not shown). Furthermore, it was demonstrated that the O_2 was quantitatively reduced to H_2O_2 by adding catalase to the reaction solution at the conclusion of the urate oxidase reaction. Catalase regenerated $47 \pm 3\%$ of the O_2 which had been utilized in the urate oxidase reaction.

Table 3: Effects of Copper and Copper Chelators on Urate Oxidase Activity[a]

treatment	relative activity
none	1.0
dialysis vs 0.5 mM $CuSO_4$	0.84
dialysis vs 0.5 mM 1,10-phenanthroline	0.98
assay in presence of 0.5 mM 1,10-phenanthroline	1.07

[a] Initial velocities were determined at 25 °C by measuring O_2 uptake.

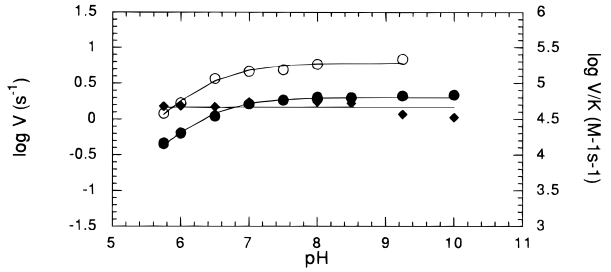

FIGURE 1: pH dependence of the kinetic parameters for the urate oxidase reaction. V (closed circles), $(V/K)_{urate}$ (open circles), $(V/K)_{O_2}$ (closed diamonds). The lines were calculated by fitting the data to eq 5. When urate was the variable substrate it was varied between 8 and 200 μM at 480 μM O_2; when O_2 was the variable substrate it was varied between 50 and 740 μM at 250 μM urate.

Steady-State Kinetic Studies. Initial velocity kinetic studies of the urate oxidase reaction were carried out at pH 9.25 by varying the urate concentration at several different fixed O_2 concentrations. These data yielded a family of intersecting lines in the reciprocal plot indicating sequential addition of the substrates to urate oxidase. There was no indication of nonlinearity in the reciprocal plots or substrate inhibition by urate. The data were fitted to eq 2 and yielded values for the K_ms of urate and O_2 of 9.8 $\pm$ 1.3 and 61 $\pm$ 5 μM, respectively; V was 3.57 $\pm$ 0.12 μmol/min/mg. The dissociation constant for urate from the binary complex (K_{iurate}) was 17 $\pm$ 4 μM; the overall quality of the fit of the data to eq 2 is given by σ, which was 0.09 μmol/min/mg. The data showed a significantly poorer fit to the model for a ping-pong reaction, yielding a σ value of 0.13 μmol/min/mg.

Table 2 summarizes the inhibition data obtained at pH 9.0−9.25. Xanthine was found to be a competitive inhibitor versus urate with a K_i of 4.5 $\pm$ 0.4 μM; xanthine was noncompetitive versus O_2. These data are consistent with ordered addition of urate to the enzyme followed by O_2. 9-Methylurate was also found to be a competitive inhibitor versus urate with a K_i of 22 $\pm$ 2 μM. Neither 1-methylurate, 3-methylurate, nor 7-methylurate exhibited significant inhibition of urate oxidase, and the limited solubility of these compounds precluded accurate determinations of their inhibition constants.

pH Dependence of the Kinetic Parameters. The pH dependence of V, $(V/K)_{urate}$, and $(V/K)_{O_2}$ for the urate oxidase reaction is shown in Figure 1. The $(V/K)_{O_2}$ profile was pH independent, but the V and $(V/K)_{urate}$ profiles showed an ionization on the acid side. The V profile defined a pK of 6.32 $\pm$ 0.02, and the $(V/K)_{urate}$ profile defined a pK of 6.37 $\pm$ 0.05. The pH dependence of 9-methylurate and xanthine inhibition was determined as well (Figure 2). The K_i for 9-methylurate was pH independent, but that for xanthine defined a pK of 7.47 $\pm$ 0.08.

Isotope Trapping. Representative mass spectra of menadione epoxide generated from enzymatically produced H_2O_2 are shown in Figure 3. The molecular ion of unlabeled

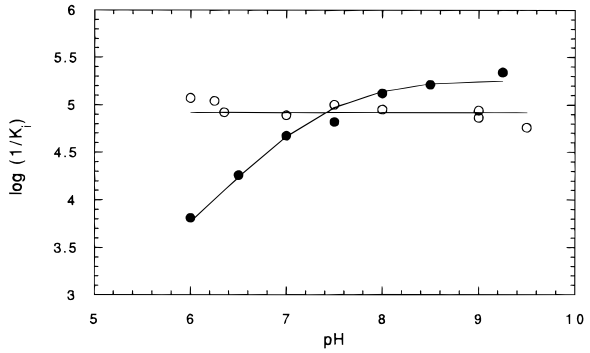

FIGURE 2: pH dependence of the inhibition of the urate oxidase reaction by 9-methylurate (open circles) and xanthine (closed circles). The data for xanthine inhibition were fitted to eq 5; the line through the 9-methylurate data was drawn to aid the eye. The K_is derived from Dixon plots were determined from experiments in which the urate concentration was 100 μM.

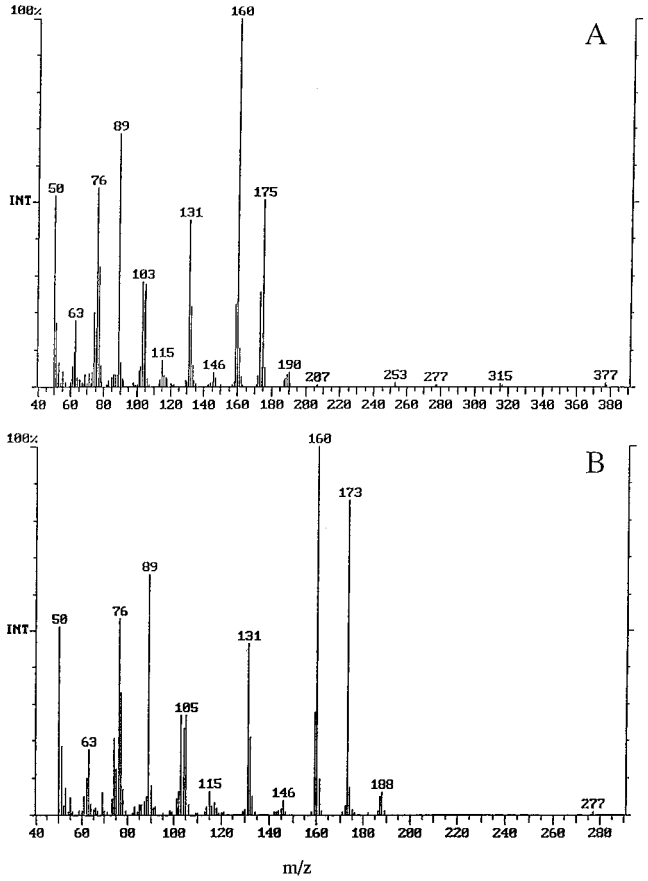

FIGURE 3: Mass spectra of menadione epoxide prepared from H_2O_2 generated by catalytic turnover of urate oxidase. (A) Reaction conducted under an atmosphere of $^{18}O_2$. The reaction contained 1.5 μmol of urate in 10 mM CHES, pH 9.0, in a volume of 5 mL and was initiated by the addition of a catalytic amount of urate oxidase; the resulting H_2O_2 was used to epoxidize menadione. (B) Isotope-trapping experiment. Menadione epoxide produced from the H_2O_2 generated in a single turnover of urate oxidase in buffer containg $^{18}O_2$ and $^{16}O_2$ as described in the text.

menadione expoxide appears at *m*/*z* 188; however, a far more intense signal at *m*/*z* 173 arises from a fragment which has lost the methyl group. When $H_2{}^{18}O_2$ is used to epoxidize menadione, the corresponding species appear at *m*/*z* 190 and 175 (Figure 3A). Because the demethylated species still bears the epoxide oxygen, the ^{18}O content of the menadione epoxide and, by extension, the enzymatically generated H_2O_2 can be inferred from the relative intensities of the peaks at *m*/*z* 173 and 175. In the isotope-trapping experiment that

was conducted, a solution containing 100 μM $^{18}O_2$ was diluted into a solution containing 1.4 mM $^{16}O_2$, so that the final percentage of $^{18}O_2$ in the solution was 1.6% of the total O_2. This relative amount of $^{18}O_2$ should be reflected in the intensities of the *m*/*z* 173 and 175 peaks in the menadione epoxide sample prepared from the aliquot removed from the reaction after 5 min of reaction. In fact, the intensity of the *m*/*z* 175 peak was 1.5% that of the *m*/*z* 173 peak, in excellent agreement with the expected result (data not shown). For the sample derived from the H_2O_2 generated in a single turnover of the enzyme, the intensity of the *m*/*z* 175 peak was 1.6% that of the *m*/*z* 173 peak, indicating that no $^{18}O_2$ was trapped on the enzyme (Figure 3B). Any amount of trapping should have resulted in ^{18}O incorporation to an extent greater than that seen in the sample prepared from H_2O_2 generated in the steady-state.

DISCUSSION

Few kinetic studies of urate oxidase have been reported in the recent literature, and earlier work presents conflicting results. Extensive studies were carried out with the porcine liver enzyme, but the data did not define the kinetic mechanism, and it was reported that substrate inhibition occurred (Baum et al., 1956). The apparent substrate inhibition was shown to be an artifact arising from the absorbance of the metastable product of the enzymatic reaction, and kinetic studies carried out monitoring the production of the transiently observable product at 312 nm yielded nonlinear reciprocal plots, which led to the proposal that substrate addition is random (Pitts & Priest, 1974). Another study of urate oxidase from *A. flavus* failed to detect O_2 binding to free enzyme under equilibrium conditions, which implies that the enzyme follows an ordered mechanism with urate binding first (Conley & Priest, 1980b). More recent studies of the soybean root nodule enzyme yielded data which did not distinguish between a sequential and a ping-pong mechanism, and the order of substrate binding was not investigated (Lucas et al., 1983).

We have investigated the kinetic mechanism of urate oxidase from soybean root nodules using an oxygen electrode to monitor the reaction in order to avoid artifacts arising from absorbance of unidentified species in solution during the course of the reaction. The data yielded linear reciprocal plots which intersected to the left of the *y*-axis, and there was no evidence of substrate inhibition by urate. The intersecting reciprocal plots indicate that substrate addition is sequential; the order of substrate addition was determined from inhibition studies. Xanthine exhibited competitive inhibition versus urate and noncompetitive inhibition versus O_2. These data are consistent with a mechanism in which urate binds to the enzyme before O_2.

Urate oxidase presents some challenges to classical kinetic studies; since the reaction is irreversible and the product is unstable, product inhibition studies are not feasible (allantoin is a very weak inhibitor of the enzyme). Although a number of purines and other compounds such as oxonate (Fridovich, 1965) are competitive inhibitors versus urate, there are no good competitive inhibitors versus O_2. Therefore, to confirm the results of the steady-state kinetic studies, we turned to isotope-trapping experiments using $^{18}O_2$. The intent of these experiments was to determine whether any evidence for a productive enzyme$-O_2$ complex could be gathered. A solution containing urate oxidase and $^{18}O_2$ was diluted into a solution containing urate and an excess of $^{16}O_2$. After approximately 1 s the reaction was quenched; the turnover number for urate oxidase is 2 s^{-1}, so only one or two catalytic cycles should have occurred before the quench. Mass spectrometric analysis revealed that the isotopic composition of the H_2O_2 generated in this experiment was the same as that of H_2O_2 generated during steady-state turnover. The conclusion from these data is that O_2 cannot bind productively to urate oxidase in the absence of urate. An alternative explanation, that O_2 adds to the free enzyme in rapid equilibrium, is not supported by the initial velocity kinetic pattern. Therefore, it appears that urate oxidase follows an ordered mechanism in which urate binding precedes O_2 binding.

The kinetic mechanism is of interest given the oxygen-dependent nature of the chemistry carried out by urate oxidase. Many oxidases such as the flavin-dependent monoamine oxidase B and the copper-containing plasma amine oxidase display ping-pong kinetics because the catalytic reactions occur in two separable half-reactions (Husain et al., 1982; Oi et al., 1970). In each case, the substrate is oxidized by the cofactor, and O_2 serves to reoxidize the cofactor after the first half-reaction has been completed. In the case of the copper-dependent amine oxidase, oxidation of the substrate results in formation of the aminoquinol form of the topaquinone cofactor, which is oxidized by O_2 in the second half-reaction to complete the catalytic cycle (Hartmann et al., 1993). In the flavin-dependent monoamine oxidase reaction, the second half-reaction is the oxidation of flavin by O_2.

However, no cofactor has been identified in urate oxidase. Although copper was reported to be present in urate oxidase from soybean root nodules in substoichiometric amounts (Bergmann et al., 1983), our own investigations have failed to reveal the presence of copper above trace levels. Samples of urate oxidase isolated from soybean root nodules and of the purified recombinant enzyme, which had essentially the same specific activity, contained less than 0.1 equiv of copper per subunit. These data rule out the presence of tightly bound copper in the purified enzyme. To determine whether urate oxidase activity was dependent on copper, which was sequestered by the enzyme from the buffer, the effect of dialysis against both copper and a copper chelator, 1,10-phenanthroline, was examined. Neither treatment resulted in a marked change in the activity of the enzyme (Table 3); furthermore, assaying the enzyme in the presence of 1,10-phenanthroline failed to have an effect on the observed activity, suggesting that the enzyme does not require copper for activity. Urate oxidases isolated from *Bacillus fastidiosus* (Bongaerts et al., 1978), *Candida utililis* (Nishimura et al., 1982), and *A. flavus* (Conley & Priest, 1980a) have been shown to be free of any transition metals.

The molecular mass of recombinant urate oxidase was measured by MALDI-TOF mass spectrometry. The measured value of 35 059.8 Da is in excellent agreement with the value of 35 052 Da, which is calculated from the deduced amino acid sequence, taking into account the fact that the N-terminal methionine is not present. These data suggest that there is not a covalently bound organic cofactor present in urate oxidase. The absorption spectrum of the purified enzyme showed no chromophores except those attributable to amino acid residues (data not shown). Some results reported in the literature on rat liver urate oxidase are also consistent with the notion that urate oxidase does not contain

any of the commonly occurring cofactors. When that protein is expressed in *E. coli*, it forms insoluble aggregates; it has been demonstrated that the aggregate can be solubilized and enzymatic activity regained by a series of washes at pH 10 and 12 (Ito et al., 1992). The success of this protocol suggests, although is by no means definitive proof, that urate oxidase is not dependent on any noncovalently bound cofactor for activity.

Neither the role of acid−base catalysts in the urate oxidase reaction nor the protonation state of urate undergoing reaction has been defined previously. The V and $(V/K)_{urate}$ profiles were very similar, showing that the protonation of a residue with a pK of ~6.3 prevented catalysis. The fact that both parameters show a similar pH dependence suggests that the protonation state of the ionizing residue is important for catalysis but not for binding (Cleland, 1977). The observed pKs do not correspond well with the first pK of urate, 5.3 (Pfleiderer, 1974), which suggests that the ionization can be assigned to a residue on the enzyme. The pH dependence of the inhibition of urate oxidase was determined in order to test this assignment further. Xanthine and 9-methylurate were potent competetive inhibitors versus urate, and the pH dependence of their K_is is shown in Figure 2. The pKs of 9-methylurate are 5.1 and 11.5 (Pfleiderer, 1974), so its ionization state did not vary across the pH range used in these studies, and its K_i is seen to be pH independent. Xanthine has a pK of 7.4, which does appear in the pK_i profile (Figure 2). Significantly, neither pK_i profile showed the pK at 6.3, confirming the suggestion that the enzyme group responsible for that pK does not participate in binding.

Because the activity of urate oxidase was difficult to measure accurately below pH 6, the ionization state of urate (pK 5.3) required for reaction could not be determined directly by pH kinetic studies. However, from the pK_i profiles, it is apparent that urate oxidase binds the inhibitors as the monoanionic species; by analogy it is likely that urate binds as the monoanion as well. There has been disagreement over whether the monoanion is deprotonated at N3 or N9 [for example, see Simic and Jovanovic (1989)]. Detailed spectroscopic studies of urate and various methylurates led Pfleiderer (1974) to suggest that N3 was the site of the first ionization.[3] In addition, the sodium salt of urate was established to be the N3-deprotonated tautomer by X-ray crystallography (Mandel & Mandel, 1976). The fact that 9-methylurate is a potent inhibitor of urate oxidase, while the other isomers of *N*-methylurate exhibit little or no inhibition, suggests that ionization at the 9-position of the purine is not required for binding. Thus, it is most likely that N3-deprotonated urate is the true substrate for urate oxidase. This species should be the most prevalent form of urate in solution at physiological pH values.

Extensive studies on the electrochemical oxidation of uric acid and urate have been conducted. Voltammetric studies of urate oxidation in aqueous solution have shown that the oxidation becomes more facile with increasing pH; a plot of the peak potential versus pH shows two breaks, at pH 5.7 and 9.8, which correspond roughly with the pKs of urate. These data led to the suggestion that the species which actually undergoes oxidation in solution is the dianion of urate (Goyal et al., 1994). The same situation may arise at the active site of urate oxidase. The pK_i profiles suggest

Scheme 1

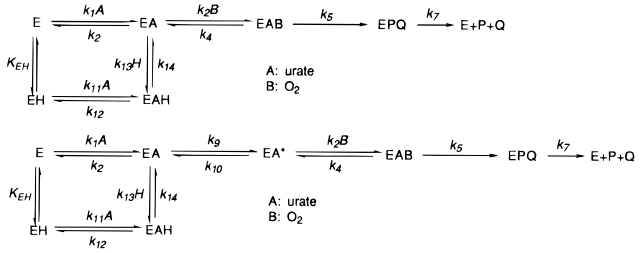

that the urate monoanion is the species which binds to the enzyme, and the V and $(V/K)_{urate}$ profiles show that a catalytic residue on the enzyme must be deprotonated for activity. The role of this residue may be to abstract a proton from urate to generate the dianion, which can be oxidized more easily than the monoanion.

In order to understand why V and $(V/K)_{urate}$ were pH dependent, but the $(V/K)_{O_2}$ profile was pH independent over the range in which experiments were conducted, we examined two models (Scheme 1). In the first model, urate and O_2 binding was ordered and protonation of the free enzyme or the enzyme−urate complex caused a loss of activity. In this mechanism, the V and $(V/K)_{urate}$ profiles are predicted to describe waves (Cleland, 1977); although the experimental data clearly do not exhibit wave shapes, it is possible that the data simply do not extend to low enough pH values for the lower plateau to become apparent. If this were the case, the lower plateau would have to be at least 10-fold lower than the high pH plateau. For V, the high and low pH plateaus are described by $k_5k_7/(k_5 + k_7)$ and $k_5k_7/[k_5k_7/k_{14} + (k_5 + k_7)]$, respectively. Thus, in order to fit the observed data, k_{14}, the rate constant for deprotonation of the EAH complex (see Scheme 1) would have to be at least 10-fold slower than the product of the rate constants describing the chemical step and product release step, which seems unlikely. For $(V/K)_{urate}$, the high and low pH plateaus are described by k_1 and $k_{11}k_{14}/(k_{12} + k_{14})$, respectively. Again, in order to conform to the observed data, the low pH plateau would have to be at least 10-fold lower than the high pH plateau. If k_{12}, the rate constant for dissociation of substrate from the EAH complex is much greater than k_{14}, the rate constant for deprotonation of the EAH complex, k_{11}/k_{12} would have to be at least 10-fold lower than k_1, the rate constant for association of substrate. If k_{12} is much less than k_{14}, then k_{11}, the rate constant for association of urate with EH, would have to be at least 10-fold lower than k_1. However, it is difficult to rationalize why the association of an anionic substrate would be slowed at least 10-fold by the protonation of an active site residue. Finally, this mechanism predicts that $(V/K)_{O_2}$ would exhibit the true pK of the EAH complex; although the observed data are pH independent, again, it is possible that the pK lies outside of the experimentally accessible range. We do not know the true value of the pK for the EAH complex so it is difficult to assess the likelihood that kinetic factors could perturb the pK beyond the pH regime in which we can work. In summary, although the first model in Scheme 1 is not mathematically eliminated from the realm of possibility, it does not seem to provide a very satisfactory explanation of the experimental data.

The second model differs from the first only by including a unimolecular step between the binding of the two substrates. In this model, the V profile is predicted to exhibit an apparent pK defined by $pK_{EAH} - \log(1 + k_9/k_7 + k_9/k_5)$;

[3] *Ab initio* calculations carried out at the MP2/6-31+G* level indicate that N3 is the site of the first ionization.[1]

$(V/K)_{urate}$ will exhibit an apparent pK at pK_{EH} − log(1 + k_9/k_2); and $(V/K)_{O_2}$ will exhibit an apparent pK at pK_{EAH} − log(1 + k_9/k_{10}). Therefore, if k_9 is large relative to k_{10}, and k_9/k_{10} is large relative to k_9/k_7 and k_9/k_5, the pK expected in the $(V/K)_{O_2}$ profile would be shifted to a lower pH value than it appears in the V profile, i.e., out of the observable range. These constraints are met by a reaction profile in which the equilibrium between EA and EA* strongly favors EA*, and the rates of chemistry and product release are faster than the forward rate of the EA isomerization; in other words, the rate of the reaction would be largely limited by the rate of the conversion of the enzyme−urate to enzyme*−urate complex before addition of O_2. In fact, this seems quite reasonable and is reminiscent of the situation observed with phenylalanine hydroxylase, in which there is no observable deuterium kinetic isotope effect from [4-^{2}H]-L-phenylalanine, and it was suggested that formation of the activated oxygen−pterin complex is the rate-limiting step (Carr et al., 1995).

The nature of the unimolecular step which the pH kinetics data seem to require is not known. It may be an isomerization of the enzyme; alternatively, it may be a step in which the catalytic base abstracts a proton from urate to generate the dianion. It has recently been suggested that lipoxygenase abstracts hydrogen from linoleic acid bound at the active site prior to O_2 binding (Glickman & Klinman, 1996); perhaps substrate activation in advance of O_2 binding is a common theme in O_2-dependent enzymes.

It is interesting to note that despite the fact that a high pH optimum has often been used as a defining characteristic of urate oxidase (Bongaerts et al., 1978; Lucas et al., 1983; Arima & Nose, 1968), the kinetic parameters reported here are constant between pH 7 and 10. The apparent high pH optimum presumably arises from the fact that the metastable product, whose appearance masks the disappearance of urate spectrophotometrically, is more stable at pH 7−8 than at higher pHs. Our data suggest that urate oxidase should be catalytically active in the somewhat acidic environment of the root nodule.

ACKNOWLEDGMENT

We are grateful to Jennifer Buddenbaum for technical assistance in the preparation of urate oxidase, Eric Gaucher for assistance in cloning the soybean urate oxidase gene, and Professor Tom Mawhinney for the GC−MS analysis of the menadione epoxide samples. MALDI-TOF mass spectrometry was provided by the Washington University Mass Spectrometry Resource, an NIH Research Resource (Grant No. P41RR0954).

SUPPORTING INFORMATION AVAILABLE

Full equations for V_{max}, $(V/K)_{urate}$ and $(V/K)_{O_2}$ for both kinetic mechanisms shown in Scheme 1 (2 pages). Ordering information is given on any current masthead page.

REFERENCES

Ames, B. N., Cathcart, R., Schwiers, E., & Hochstein, P. (1981) *Proc. Natl. Acad. Sci. U.S.A. 78*, 6858−6862.

Arima, K., & Nose, K. (1968) *Biochim. Biophys. Acta 151*, 54−62.

Atkins, C. A., Sanford, P. J., Storer, P. J., & Pate, J. S. (1988) *Plant Physiol. 88*, 1229−1234.

Baum, H., Hubscher, G., & Mahler, H. R. (1956) *Biochim. Biophys. Acta 22*, 514−527.

Bergmann, H., Preddie, E., & Verma, D. P. S. (1983) *EMBO J. 2*, 2333−2339.

Bongaerts, G. P. A., & Vogels, G. D. (1979) *Biochim. Biophys. Acta 567*, 295−308.

Bongaerts, G. P. A., Uitzetter, J., Brouns, R., & Vogels, G. D. (1978) *Biochim. Biophys. Acta 527*, 348−358.

Carr, R. T., Balasubramanian, S., Hawkins, P. C. D., & Benkovic, S. J. (1995) *Biochemistry 34*, 7525−7532.

Cleland, W. W. (1977) *Adv. Enzymol. Relat. Areas Mol. Biol. 45*, 273−387.

Cleland, W. W. (1979) *Methods Enzymol. 63*, 103−138.

Conley, T. G., & Priest, D. G. (1980a) *Biochem. J. 187*, 727−732.

Conley, T. G., & Priest, D. G. (1980b) *Biochem. J. 187*, 733−738.

Fridovich, I. (1965) *J. Biol. Chem. 240*, 2491−2494.

Glickman, M. H., & Klinman, J. P. (1996) *Biochemistry 35*, 12882−12892.

Goyal, R. N., Mittal, A., & Agarwal, D. (1994) *Can. J. Chem. 72*, 1668−1674.

Hartmann, C., Brzovic, P., & Klinman, J. P. (1993) *Biochemistry 32*, 2234−2241.

Husain, M., Edmondson, D. E., & Singer, T. P. (1982) *Biochemistry 21*, 595−600.

Ito, M., Kato, S., Nakamura, M., Go, M., & Takagi, Y. (1992) *Biochem. Biophys. Res. Commun. 187*, 101−107.

Kaltwasser, H. (1971) *J. Bacteriol. 107*, 780−786.

Karr, D. B., Waters, J. K., Suzuki, F., & Emerich, D. W. (1984) *Plant Physiol. 75*, 1158−1162.

Keilin, D., & Hartree, E. F. (1936) *Proc. R. Soc. London, Ser. B 119*, 114−140.

Layzell, D. B., & LaRue, T. A. (1982) *Plant Physiol. 70*, 1290−1298.

Lee, N.-G., Stein, B., Suzuki, H., & Verma, D. P. S. (1993) *Plant J. 3*, 599−606.

Lucas, K., Boland, M. J., & Schubert, K. R. (1983) *Arch. Biochem. Biophys. 226*, 190−197.

Mahler, H. R., Hubscher, G., & Baum, H. (1955) *J. Biol. Chem. 216*, 625−641.

Mandel, N. S., & Mandel, G. S. (1976) *J. Am. Chem. Soc. 98*, 2319−2323.

Maples, K. R., & Mason, R. P. (1988) *J. Biol. Chem. 263*, 1709−1712.

Massey, V. (1994) *J. Biol. Chem. 269*, 22459−22462.

McClure, P. R., & Israel, D. W. (1979) *Plant Physiol. 64*, 411−416.

Modric, N., Derome, A. E., Ashcroft, S. J. H., & Poje, M. (1992) *Tetrahedron Lett. 33*, 6691−6694.

Nishimura, H., Yoshida, K., Yokota, Y., Matsushima, A., & Inada, Y. (1982) *J. Biochem. 91*, 41−48.

Oi, S., Inamasu, M., & Yasumobu, K. T. (1970) *Biochemistry 9*, 3378−3383

Ortiz de Montellano, P., & Catalano, C. E. (1985) *J. Biol. Chem. 260*, 9265−9271.

Pfleiderer, W. (1974) *Liebigs Ann. Chem.* 2030−2045.

Pitts, O. M., & Priest, D. G. (1974) *Arch. Biochem. Biophys. 163*, 359−366.

Reynolds, P. H. S., Boland, M. J., Blevins, D. G., Randall, D. D., & Schubert, K. R. (1982) *Trends Biochem. Sci.* 366−368.

Schuler, W., & Reindel. W. (1933) *Z. Physiol. Chem. 215*, 258−266.

Segel, I. R. (1975) *Enzyme Kinetics*, John Wiley & Sons, New York.

Sevanian, A., Davies, K. J. A., & Hochstein, P. (1991) *Am. J. Clin. Nutr. 54*, 1129S−1134S.

Simic, M. G., & Jovanovic, S. V. (1989) *J. Am. Chem. Soc. 111*, 5778−5782.

Snatzke, G. (1980) *J. Org. Chem. 45*, 4094−4096.

Suzuki, H., & Verma, D. P. S. (1991) *Plant Physiol. 95*, 384−389.

Wu, X., Muzny, D. M., Lee, C. C., & Caskey, C. T. (1992) *J. Mol. Evol. 34*, 78−84.

BI963184W